Molecular Crystals and Liquid Crystals

ISSN: 1542-1406 (Print) 1563-5287 (Online) Journal homepage: http://www.tandfonline.com/loi/gmcl20

Electrical Stabilities of In_2O_3-ZnO-SnO_2 (IZTO) Films Against the External Stresses

Changhyun Lee, Kang Bae, Jaeyoung Ha, Hwamin Kim, Sunyoung Sohn & Sungbo Seo

To cite this article: Changhyun Lee, Kang Bae, Jaeyoung Ha, Hwamin Kim, Sunyoung Sohn & Sungbo Seo (2016) Electrical Stabilities of In_2O_3-ZnO-SnO_2 (IZTO) Films Against the External Stresses, Molecular Crystals and Liquid Crystals, 626:1, 246-253, DOI: 10.1080/15421406.2015.1076295

To link to this article: http://dx.doi.org/10.1080/15421406.2015.1076295

Published online: 22 Mar 2016.

Submit your article to this journal

Article views: 29

View related articles

View Crossmark data

Full Terms & Conditions of access and use can be found at
http://www.tandfonline.com/action/journalInformation?journalCode=gmcl20

Download by: [College of Business Education] **Date:** 22 December 2016, At: 13:20

MOLECULAR CRYSTALS AND LIQUID CRYSTALS
2016, VOL. 626, 246–253
http://dx.doi.org/10.1080/15421406.2015.1076295

Taylor & Francis
Taylor & Francis Group

Electrical Stabilities of In_2O_3-ZnO-SnO_2 (IZTO) Films Against the External Stresses

Changhyun Lee[a], Kang Bae[a], Jaeyoung Ha[a], Hwamin Kim[b], Sunyoung Sohn[c], and Sungbo Seo[a]

[a]Department of Electronics and Display Engineering, Catholic University of Daegu, Gyeongsan, Republic of Korea; [b]Department of Advanced Materials and Chemical Engineering, Catholic University of Daegu, Gyeongsan, Republic of Korea; [c]Department of Creative IT Engineering, Pohang University of Science and Technology, Pohang, Republic of Korea

ABSTRACT

The $(In_2O_3)_{77.34}(ZnO)_x(SnO_2)_{22.66-x}$ (denote to IZTO-2) films with x = 13, 15, 17, 19 wt.% were prepared on PET film with a 100-nm-thick SiO_2 buffer layer by using RF-magnetron sputtering method, and their electrical stabilities were tested under various external stresses such as moist heat, temperature fluctuations and bending of substrate films. The lowest resistivity of 4.8×10^{-4} Ω•cm was observed in the IZTO-2 film of x = 17 wt.% which also had such good properties as high electrical stability, surface uniformity, and high conductivity as compared with those of another $(In_2O_3)_{90}(ZnO)_7(SnO_2)_3$ (IZTO-1) film. These results suggest that the optimum starting composition for IZTO film with high quality as a flexible transparent conducting oxide(TCO) film is In_2O_3 : ZnO : SnO_2 = 77.34 : 17 : 5.66 wt.%. The electrical stability of the optimum IZTO-2 film was greatly improved because the SiO_2 buffer layer introduced between IZTO thin film and PET substrate acted as a blocking barrier to water vapour and organic solvents diffusing from the PET film and also as a buffer layer withstanding the bending damage.

KEYWORDS

Thin Film; Reactive Mode; TCO; Flexibility; IZTO

Introduction

At present the In_2O_3-SnO_2 (ITO) thin films deposited by using a sputtering method are most commonly used as transparent conducting oxide (TCO) thin films for optoelectronics devices such as touch panels, flat panel displays (FPDs) and thin-film solar cells [1–15]. ITO film has also been used as an electrode in a-Si solar cell of supersaturates type, but some problems have been reported such as high deposition temperature, instability under hydrogen plasma atmosphere, and rough surface [16–20]. Recently, In_2O_3-ZnO (IZO) and In_2O_3-ZnO-SnO_2 (IZTO) thin films have been actively investigated due to the good optical and electrical properties comparable to the ITO films [21–27]. Although the electrical properties and chemical stabilities of the multi-component oxide thin films are highly dependent on their compositions, their effect on the composition of the thin films have not been well known. We examined IZTO films with the composition ratio of $(In_2O_3)_{90}(ZnO)_x(SnO_2)_{10-x}$ and reported that

CONTACT Sungbo Seo kzaleil@cu.ac.kr Catholic University of Daegu, Hayang, Gyeongbuk, 712–702, Korea (ROK)
This paper was originally submitted to *Molecular Crystals and Liquid Crystals*, Volume 617, Proceedings of the 18th International Symposium on Advanced Display Materials and Devices.
Color versions of one or more of the figures in the article can be found online at www.tandfonline.com/gmcl.
© 2016 Taylor & Francis Group, LLC

IZTO film with a specific composition ratio of In_2O_3 : ZnO : SnO_2 = 90 : 7: 3 wt.% (denote to IZTO-1 film) showed good chemical stability with high electric conductivity, high transmittance and particularly strong adhesion to the substrates. This composition ratios were based on the optimum composition ratio (In_2O_3 : ZnO = 90 : 10 wt.%) of ITO thin films [28–30].

In this work, we investigated IZTO thin films with another composition ratio of $(In_2O_3)_{77.34}(ZnO)_x(SnO_2)_{22.66\text{-}x}$ (denote to IZTO-2 films) based on the optimum composition ratio (In_2O_3 : ZnO = 77.34 : 22.66 wt.%) of IZO film [29] and compared their properties with those of IZTO-1 film. Since most plastic films contain water vapor or organic solvents, mixing of the vaporized gases in the sputtering process affects the properties of the deposited IZTO films. We therefore investigated electrical and the mechanical stabilities against external stresses such as moist heat, temperature variation, and bending of substrate films for the IZTO-2 films deposited on PET film with a SiO_2 buffer layer. The results were compared with those of IZTO-1 film.

Experimental methods

The composite powders of IZTO-2 (x = 13∼19 wt.%) were mixed by using ball mill for 24hours with additional hand milling and were calcined at 1000°C for two hours to remove the moisture. The 2-inch targets were made under a pressure of 12 tons by using a Caver press and were solidified for one hour at 600°C in vacuum of 10^{-5} Torr. These sintered pellets were used as the sputter targets for IZTO-2 films. The IZTO-2 films were deposited on flexible PET substrates at room temperature by using a conventional rf-magnetron sputtering method. The PET(Dupont ST504) was obtained by using solid-state polycondensation had 0.7−0.8 dl/g at a water vapor transmission rate of 4.2 g/cm^2/day and glass transition temperature of 80°C the solid state took about 15 to 20 hours to achieve at 210°C. Thus, the PET with a contraction rate below 0.1% was thermally very stable at 150°C. The sputtering depositions of IZTO-1 and IZTO-2 with various composition ratios were carried out at room temperature in a pure Ar gas at a working pressure of 2×10^{-3} Torr and an rf-power of 75 W. To make a buffer layer, we pre-coated SiO_2 with a thickness of 100 nm on the PET substrate by using an ion-gun-assisted sputtering method. The PET substrate with a size of 50×50 mm^2 was placed parallel to the target surface at a distance of 8.5 cm during the deposition.

On the other hand, in a case of IZTO-1 films, we prepared only one film with a composition of $(In_2O_3)_{90}(ZnO)_7(SnO_2)_3$ that is known to show the most excellent electrical and chemical stabilities against the moist heat [25, 27]. IZTO-1 and IZTO-2 films were prepared under the same sputtering conditions. In order to examine the stability of IZTO films in a practical living environment, we imposed three specific thermal and moist stresses on the as-deposited films: (i) a low temperature of −25°C or (ii) a high temperature of 100°C repeated thermal stresses due to violent temperature switching between quenching at −25°C and annealing at 100°C for 5 min for each process, and (iii) a moist-heat condition at 90% relative humidity (RH) at 80°C. Also, in the test of bending effect for IZTO films, the substrates were bent around a cylinder of radius 18 mm or 20 mm. The stress effects of the films are investigated by measuring variation in their sheet resistance before and after imposition of the stresses. Surface morphology of the IZTO films was observed by using an atomic force microscope (AFM) and a scanning electron microscope (SEM). The film thickness was measured by using an α-step profiler and an ellipsometer. The four-point probe methods were used to measure the sheet resistance of the films.

Results and discussion

In Fig. 1(a), we plot the electrical resistivity (ρ), the carrier concentration (n), and the Hall mobility (μ) as functions of the ZnO content for 150-nm-thick IZTO-2 films deposited at room temperature on PET substrate. The resistivity of IZTO-2 films decreases with increasing x up to x = 17wt.%, but over x = 17 wt.%, the resistivity increases again. The lowest resistivity of 4.8×10^{-4} Ω•cm and the maximum carrier concentration of $3.2 \times 10^{20}/cm^3$ were obtained in IZTO-2 film of x = 17 wt.%, the Hall mobilities were distributed from 42 to 48 $cm^2 \cdot V^{-1} \cdot s^{-1}$ for IZTO-2 films. For reference; the resistivity of IZTO-1 film was confirmed to be 5.3×10^{-4} Ω•cm in the previous work [27].

The sheet resistance of the IZTO-2 film of x = 17 wt.% with a buffer layer is shown in Fig. 1(b) as a function of the film thickness. For comparison, that of IZTO-2 film of x = 17 wt.%

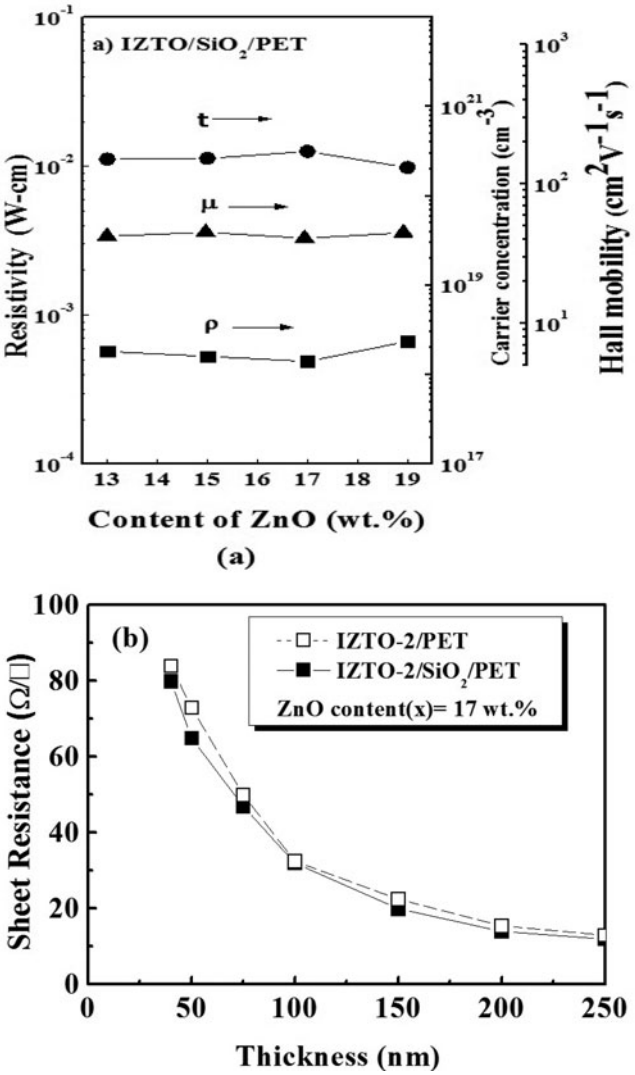

Figure 1. (a) Resistivity (ρ), carrier concentration (n), and Hall mobility (μ) of the IZTO-2 films with various the composition ratios and (b) sheet resistance of the IZTO-2(x = 17 wt.%) films with and without a buffer layer as functions of the film thickness.

without a buffer layer is also shown. The sheet resistance rapidly decreases with increasing thickness in both the films with and without the buffer layer. In general, the sheet resistance R is inversely proportional to the thickness ($R = \rho/t$, where t is the film thickness). The lower resistivity of the IZTO/SiO_2/PET sample is mainly contributed to the excellent surface uniformity caused by the inserted layers of SiO_2 because the buffer layer acts as a blocking barrier to water vapor or organic solvents diffusing from the PET substrate during deposition. It was found that the introduction of the buffer layer did not to affect seriously the electrical conductivity itself, but improved remarkably the stability of the film against external stresses, such as the moisture, the heat, and the substrate bending, as described below.

Figure 2 shows variations of the sheet resistance under a thermal stress of quenching at −25°C for 150-nm-thick IZTO-2 films deposited on the PET substrates with a SiO_2 buffer layer. It is shown that IZTO-2 film of x = 17wt.% is the most conductive compared to other films (x = 13, 15, 19 wt.%). It is also shown that all IZTO-2 films are very stable under a thermal stress of quenching at −25°C. For instance, all films show variation below 1% in their sheet resistance after being quenched for 240 h.

In Fig. 2 we also show the variation (open circles) of the sheet resistance for IZTO-1 film with a buffer layer under a thermal stress of quenching at −25°C. The IZTO-2 film with x = 17 wt.% shows a lower sheet resistance of 31.9 Ω/□ than that 37.9 Ω/□ of IZTO-1 film before the stress and IZTO-2 film is electrically more stable than IZTO-1 film. For instance, the sheet resistance of IZTO-2 film increases only by 0.8%, while IZTO-1 film increases by 5.5% after being quenched for 240h.

Figure 3 shows the annealing-time dependence of the sheet resistances under a thermal stress of heat treatment at 100°C in air for 150-nm-thick IZTO-2 films deposited on PET substrate with a SiO_2 buffer layer. As the annealing time increases, the sheet resistance of IZTO-2 film with x = 17 wt.% is almost constant, but the resistance rises monotonically for other films (x = 13, 15, 19 wt.%). After annealing for 240 h, the sheet resistance increases from 30% to 90% for IZTO-2 films with x = 13, 15, 19 wt.%, but increases only by 5.5% for the film of x = 17 wt.%.

On the other hand, for comparison, the variation of sheet resistance of IZTO-1 film under a thermal stress of heat treatment at 100°C in air is also shown in Figure 3. IZTO-2 film of

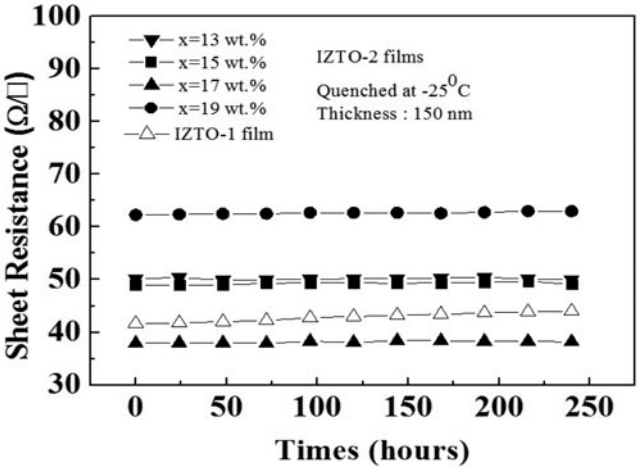

Figure 2. The sheet resistance changes as a function of the quenching time during quenching at −25°C for the 150-nm-thick IZTO-2 films of different compositions with a SiO_2 buffer layer. For comparison, those of IZTO-1 film are also shown (open circles).

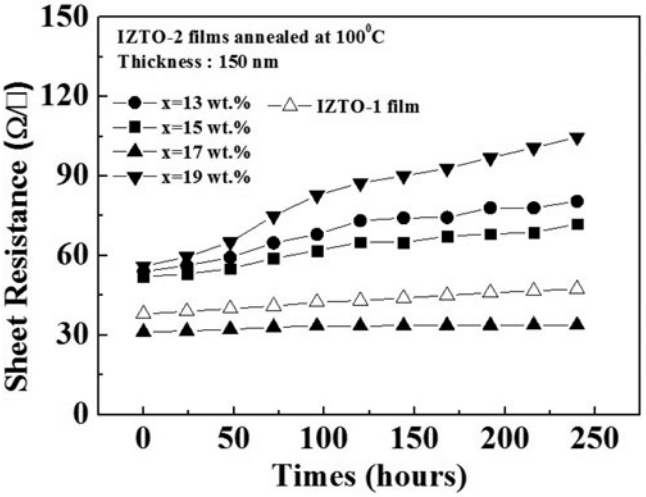

Figure 3. Variations of the sheet resistance as a function of the annealing time during the annealing at 100°C for the 150-nm-thick IZTO-2 films of different compositions with a SiO_2 buffer layer. For comparison, the variation (open circles) of IZTO-1 film is also shown.

x = 17 wt.% shows the superior electrical stability than that of IZTO-1 film, which the sheet resistance of IZTO-1 film increased up to 63% after annealing for 240h.

Figure 4 we plot the variations of the sheet resistance of the IZTO films under more severe stress: The IZTO films suffered a thermal stress in which a contrasting temperature cycles repeatedly occurred due to quenching at −25°C and annealing at 100°C for 5 min at each process. Against the thermal stress of the repeated cyclic processes, all IZTO-2 films show a comparative stable electrical characteristic. In particular, IZTO-2 film of x = 17 wt.% shows an excellent electrical stability with a variation less than 0.3%, from 31.9 to 32 Ω/□. This is much better than that(open circles) of IZTO-1 film, as shown in Fig. 4, against the same severe stresses, IZTO-1 film responds with a considerable variation of 11.8%, from 37.9 to 42.4 Ω/□.

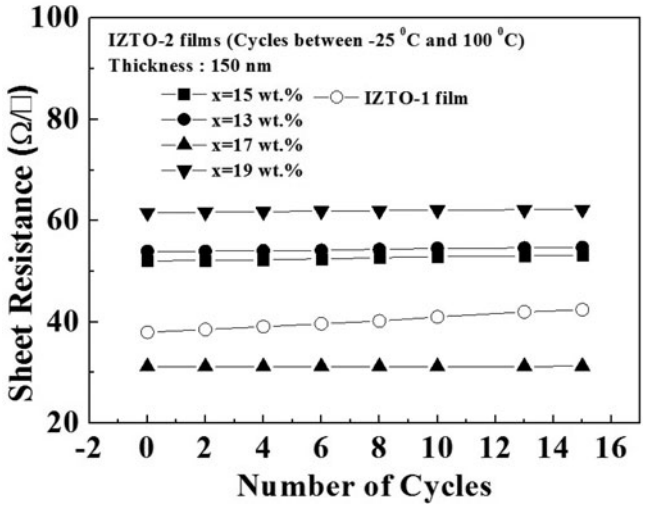

Figure 4. Changes of the sheet resistances on the repeated number of the violent temperature switching between quenching at –25°C and annealing at 100°C for IZTO-2 films with a SiO_2 buffer layer. For comparison, the change(open circles) of the sheet resistance on the thermal cyclic stress for IZTO-1 film is also shown.

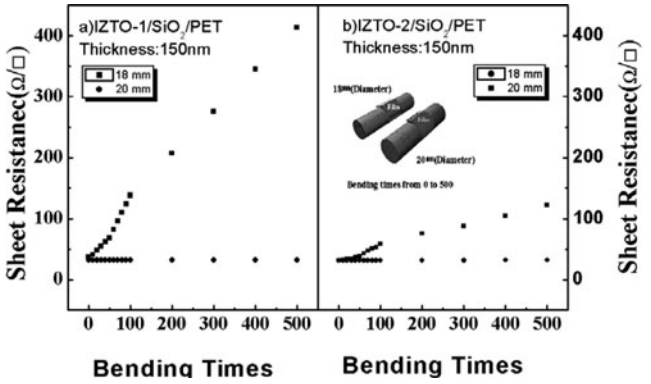

Figure 5. Variation of sheet resistance as a function of bending times for (a) IZTO-1 film and (b) IZTO-2 film of x = 17 wt.% with a SiO_2 buffer layer.

In Fig. 5, we plot the sheet resistance change as a function of bending times for (a) IZTO-1 and (b) IZTO-2 films with a thickness of 150 nm deposited on PET with a SiO_2 barrier layer. Here, the PET substrates were positively bent around a cylinder with a diameter of 18 mm and 20 mm, respectively. When the bending radius is 20 mm, the variation in the sheet resistance of IZTO-1 film is not observed, as shown in Fig. 5(a). However, in a case of the bending diameter of 18 mm, the sheet resistance of IZTO-1 film rapidly increases with increasing bending times. This variation in the sheet resistance to bending largely occurs at bending time less than 100 times, and the variation rate significantly decreases at bendings over 100 times. As shown in Fig. 5(b), the variation in the sheet resistance of IZTO-2 film show trends similar to those of IZTO-1 film, but the variation of IZTO-2 film is much less than that of IZTO-1 film in the bending with a diameter of 18 mm. Therefore, IZTO-2 film is found to be more stable than IZTO-1 film against the bending stress, and the critical bending diameter to secure flexibility is also found to be over 18 mm for the IZTO films with a thickness of about 150 nm.

Because the surface uniformity of the TCO films is a very important for ensuring a long life time of optical devices, the AFM images and XRD patterns of the as deposited IZTO films on PET substrates and their spectra of section analysis are shown in Fig. 6. A close-packed columnar structure of sharp tips is observed in the surface morphology of the IZTO-2/PET film, as shown in Fig. 6(a). The root-mean-square (RMS) value of the IZTO-2/PET film is estimated as 1.041 nm, which is a detailed average of the surface roughness and is evaluated from the section analysis of the AFM images of the film surfaces. In Fig. 6(b), however, the IZTO-2/SiO_2/PET with a buffer layer has a smoother and more uniform surface with an RMS value of 0.551 nm, which means that the SiO_2 layer contributes to the uniformity of the film in the process of deposition. For comparison, AFM image and the section analysis of IZTO-1 film with a buffer layer are also shown in Fig. 6(c). It is found that IZTO-2 films have excellent surface uniformity in comparison with IZTO-1 film. Therefore, we can guess that IZTO films are more uniformed as the relative proportions of Sn to Zn (Sn/Zn) decreases.

On the other hand, the Fig. 6(b), shows a XRD patterns for as deposited IZTO-2 films with a SiO_2 buffer layer. For comparison, that of IZTO-1 film with the buffer layer is also shown. The X-rays are injected perpendicularly to the deposited IZTO layer. There are not observed any crystalline peaks except peak at near $2\theta = 27^0$ in all films. The peak at near $2\theta = 27^0$ was identified to be peak due to the hard coating layer pre-coated on PET(Dupont ST504), as shown in previous work [22]. Therefore, IZTO films deposited on PET has amorphous structures.

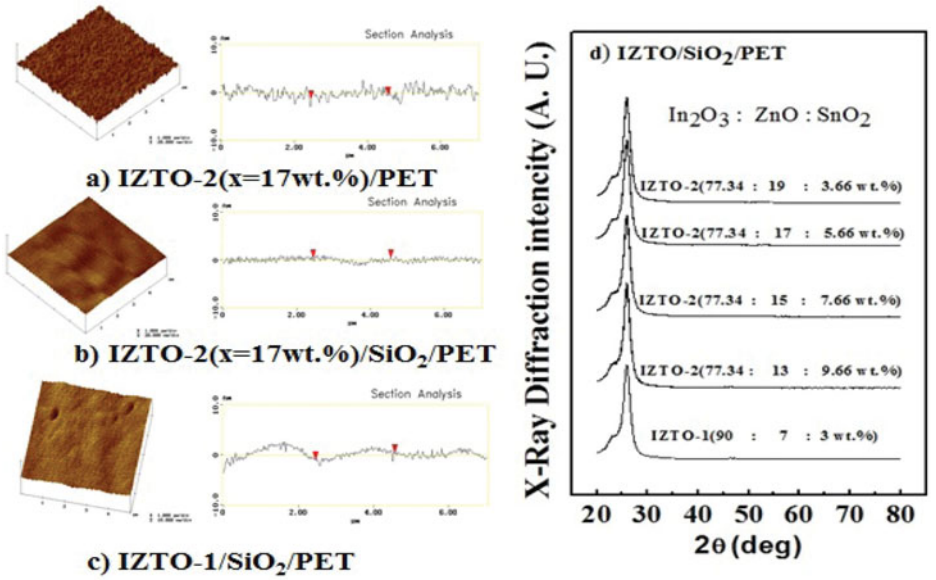

Figure 6. Typical AFM images and their spectra of section analysis for IZTO-2 film of x = 17wt.%, (a)without and (b) with a buffer layer, (c) IZTO-1 film with a buffer layer, and (d) XRD patterns of IZTO-1 film and IZTO-2 films with a buffer layer.

Conclusion

In this work, IZTO-2 thin films of $(In_2O_3)_{77.34}(ZnO)_x(SnO_2)_{22.66-x}$ with x = 13, 15, 17, 19 wt.% were prepared on PET with a SiO_2 buffer layer by using rf-magnetron sputtering method, and their electrical stabilities under various external stresses such as the moist heat, temperature fluctuations and bending of substrate films. We found that IZTO-2 film with x = 17 wt.% had better electrical stability, surface uniformity and electrical conductivity than those of IZTO-1, $(In_2O_3)_{90}(ZnO)_7(SnO_2)_3$ thin film. These results suggest that the optimum initial composition ratio of IZTO thin film is In_2O_3 : ZnO; SnO_2 = 77.34 : 17 : 5.66 wt.%. We also found that the electrical stability is greatly improved with the SiO_2 buffer layer between IZTO thin film and PET substrate, which act as a blocking barrier to water and organic vapour diffusing from the PET substrate.

Acknowledgment

This research was financially supported by the Ministry of Education (MOE) and National Research Foundation of Korea (NRF) through the Human Resource Training Project for Regional Innovation (NO. 2012026226).

References

[1] Minami, T., Kakumu, T., & Takata, S. (1996). *J. Vac. Sci. Technol. A*, *14*, 1704.
[2] Hiramatsu, H., Seo, W. S., & Koumoto, K. (1998). *Chem. Mater.*, *10*, 3033.
[3] Yan, Y., Pennycook, S. J., Dai, J., Chang, R. P. H., Wang, A., & Marks, T. J. (1998). *Appl. Phys. Lett.*, *73*, 2585.
[4] Minami, T. (1999). *J. Vac. Sci. Technol. A*, *17*, 1765.
[5] Minami, T., Miyata, T., & Yamamoto, T. (1999). *J. Vac. Sci. Technol. A*, *1*, 1822.
[6] Chopra, K. L., Major, S., & Pandya, D. K. (1983). *Thin Solid Films*, *102*, 1.

[7] Takata, S., Minami, T., & Nanto, H. (1986). *Thin Solid Films*, *135*, 183.
[8] Minami, T., Takata, S., Kakumu, T., & Sonohara, H. (1995). *Thin Solid Films*, *270*, 22.
[9] Minami, T., Sonohara, H., Kakumu, T., & Takata, S. (1995). *Jpn. J. Appl. Phys.*, *34*, L971.
[10] Park, S. H., Kim, H. M., Rhee, B. R., & Gho, E. Y. (2001). *Jpn. J. Appl. Phys.*, *40*, 1429.
[11] Manifacier, J. C., Gasiot, J., & Fillard, J. P. (1976). *J. Phys. E*, *9*, 1002.
[12] Hsiung, J. E. (1990). *J. Electron. Mater.*, *25*, 1806.
[13] Tao, G. (1994). *Energy Mater. Sol. Cell.*, *34*, 359.
[14] Kaijou et al. (1999). *United States Patent, Patent No. 5*, *972*, 527.
[15] Wen, S. J., Campet, G., Portier, J., Couturier, G., & Goodenough, J. B. (1992). *Sci. Eng.*, *115*, B14.
[16] Chopra, K. L., & Pandya, D. K. (1983). *Thin Solid Films*, *102*, 1.
[17] Takada, S., Minami, T., & Nanto, H. (1986). *Thin Solid Films*, *135*, 183.
[18] Pei, Z. L., Sun, C., Tan, M. H., Xiao, J. Q., Huang, R. F., & Wen, L. S. (2001). *J. Appl. Phys.*, *907*, 3432.
[19] Tabuchi, K., Wenas, W. W., Yamada, A., & Kakahashi, K. (1993). *Jpn. J. Appl. Phys.*, *132*, 3764.
[20] An, I., Lu, Y., Wronski, C. R., & Collins, R. W. (1994). *Appl. Phys. Lett.*, *64*, 3317.
[21] Kim, H. M. (2008). *J. Korean Phys. Soc.*, *53*, 6, 3307.
[22] Kim, H.-M., Jeung, S.-K., Ahn, J.-S., Kang, Y.-J., & Je, C.-K. (2003). *Jpn. J. Appl. Phys.*, *42*, 223.
[23] Lee, J.-K., Kim, H.-M., Park, S.-H., Kim, J.-J., Rhee, B.-R., & Shon, S.-H. (2002). *J. Appl. Phys.*, *92*, 95761.
[24] Hong, J.-S., Rhee, B.-R., Kim, H.-M., Je, K.-C., Khang, Y.-J., & Ahn, J.-S. (2004). *Thin Solid Films*, *467*, 158.
[25] Sohn, S.-Y., Kim, H.-M., Park, S.-H., & Kim, J.-J. (2004). *J. Korean Phys. Soc.*, *45*, S732.
[26] Park, S.-H., Kim, H.-M., Rhee, B.-R., Gho, E.-Y., & Shon, S.-H. (2001). *Jpn. J. Appl. Phys.*, *40*, 1429.
[27] Woo, B.-J., Hong, J.-S., Kim, S.-T., Kim, H.-M., Park, S.-H., Kim, J.-J., & Ahn, J-S. (2006). *J. Korean Phys Soc.*, *48*, 6, 1579.
[28] Phillips, J. M., Cava, R. J., Thomas, G. A., Carter, S. A., Kwo, J., Siegrist, T., Krajewski, J. J., Marshall, J. H., Peck, W. F., Jr., & Rapkine, D. H. (1995). *Appl. Phys. Lett.*, *67*, 2246.
[29] Noda, K., Sato, H., Itaya, H., & Yamada, M. (2003). *Jpn. J. Appl. Phys.*, *42*, 217.
[30] Park, J. M ., Hong, J. S., Yang, J. Y., Kim, J. J., Park, S. H ., Kim, H. M., & Ahn, J. S. (2006). *J. Korean Phys Soc.*, *48*, 6, 1530.